BER and Optimal Power Allocation for Amplify-and-Forward Relaying Using Pilot-Aided Maximum Likelihood Estimation

Kezhi Wang, *Student Member, IEEE,* Yunfei Chen, *Senior Member, IEEE,* Mohamed-Slim Alouini, *Fellow, IEEE,* and Feng Xu

Abstract—Bit error rate (BER) and outage probability for amplify-and-forward (AF) relaying systems with two different channel estimation methods, disintegrated channel estimation and cascaded channel estimation, using pilot-aided maximum likelihood method in slowly fading Rayleigh channels are derived. Based on the BERs, the optimal values of pilot power under the total transmitting power constraints at the source and the optimal values of pilot power under the total transmitting power constraints at the relay are obtained, separately. Moreover, the optimal power allocation between the pilot power at the source, the pilot power at the relay, the data power at the source and the data power at the relay are obtained when their total transmitting power is fixed. Numerical results show that the derived BER expressions match with the simulation results. They also show that the proposed systems with optimal power allocation outperform the conventional systems without power allocation under the same other conditions. In some cases, the gain could be as large as several dB's in effective signal-to-noise ratio.

Index Terms—Amplify-and-forward, cascaded channel estimation, disintegrated channel estimation, maximum likelihood, optimal power allocation, pilot-symbol-aided.

I. INTRODUCTION

DUAL-HOP transmission has been commonly used in cooperative wireless communications [1]–[9]. It can be mainly categorized into: decode-and-forward (DF) and amplify-and-forward (AF) [1]. In DF systems, the relay decodes the received signal from the source and retransmits the re-encoded signal to the destination, while in AF systems, the relay simply forwards a scaled version of the received signal to the destination with an amplification gain [1]. Depending on the nature and complexity of the AF relays, the amplification gain of AF relay can be classified as variable gain or fixed gain [3], [4]. A variable gain AF relay requires the instantaneous

K. Wang and Y. Chen are with the School of Engineering, University of Warwick, CV4 7AL Coventry, U.K. (e-mails: {Kezhi.Wang, Yunfei.Chen}@warwick.ac.uk).

M.-S. Alouini is with the Computer, Electrical and Mathematical Sciences and Engineering (CEMSE) Division, King Abdullah University of Science and Technology (KAUST), Thuwal, Makkah Province, Saudi Arabia (e-mail: slim.alouini@kaust.edu.sa).

F. Xu is with College of Computer and Information, Hohai University, Nanjing, China (e-mail: xufeng@hhu.edu.cn).

channel state information (CSI) of the first hop while a fixed gain AF relay does not need the instantaneous CSI of the first hop. Although a fixed gain relay is not expected to perform as well as a variable gain relay, it has lower energy consumption due to the saved power on the acquisition of the instantaneous CSI at the relay.

In practice, CSI is often acquired by estimation which can be performed by using either unknown or known symbols [10]. Pilot-symbol-aided system was proposed to obtain CSI using known symbols [11]. For example, linear minimum mean squared error (LMMSE) channel estimation with pilot symbols for AF relaying was studied in [7], [12], [13]. In a variable gain AF, the instantaneous CSI can be estimated both at the relay in order to determine the variable gain and at the destination for coherent demodulation, separately. This is termed as disintegrated channel estimation (DCE), as was studied in [5], [7]. Unlike a variable gain AF, in a fixed gain AF, since no CSI is required at the relay, only a cascaded channel estimation (CCE) consisting of both the source-to-relay link and the relay-to-destination link can be used to estimate CSI at the destination [5], [7]–[9], [14].

In all the aforementioned works, the estimation accuracy or the performance of the channel estimator were considered assuming unlimited power, while in practice the total power is often limited such that an optimal power allocation for pilots may be required. The authors in [15] used outage probability as a measure to obtain the optimal power allocation and they considered the allocation between training and data symbols under the total transmitting power constraint at the source but did not consider the power allocation at the relay. However, the relay is usually complexity- and power-limited. Therefore, optimal power allocation at the relay is equally important and cannot be ignored. The authors in [16] considered the power allocation between training and data symbols both at the relay and at the source using a signal-to-noise ratio (SNR) measure. However, it was reported in [17] that power allocation scheme using BER measure often achieves considerable BER performance gain over that using SNR measure, when the relay is closer to the source than to the destination. Moreover, [16] considered two power constraints: a total transmit power constraints between source and relay as well as individual power constraints at source and relay, respectively. The former can be applied in the case when the total power saving is more important, such as fixed nodes which can be charged,

while the latter can be used in the case when the individual battery power or the individual lifetime is more important, such as moving nodes. The authors in [18] also considered similar power allocation between training and data symbols as in [16] but used outage probability measure instead. Since further integral on SNR is needed, derivations of BER and outage probability are often more difficult than that of SNR in most AF systems. Therefore, one can choose to obtain the optimal power allocation according to the application and the complexity of the AF system using the specific measure, such as SNR, outage probability or BER. Moreover, the authors in [15], [16] and [18] all considered the case when the signal experiences fast fading such that LMMSE is necessary and must be used in channel estimation. In this case, the system model is so complex such that derivations of SNR, outage probability or BER using channel estimates are very difficult, if not impossible. As a result, power allocations based on SNR, outage probability or BER often do not have closed-form in this case.

However, in many previous works [19], [20] and in high data-rate applications [21], the channel coherence time is much larger than the bit interval such that the signal only experiences slow or even block fading. In this case, since the channel gain is not time-varying, maximum likelihood (ML) estimation with a much simplified structure is more suitable to obtain the channel estimates [22]. To the best of the authors' knowledge, none of the works in the literature have considered the optimal power allocation for AF relaying in the slowly fading channel using ML esimation.

In this work, we consider the optimal power allocation for AF relaying system in slowly fading Rayleigh channel using pilot-symbol-aided ML channel estimation. Our contributions can be summarized as follows:

• We first introduce the pilot-symbol-aided ML estimation method for both DCE and CCE. For DCE, we consider the case when the fading gain is estimated at the relay as well as the case when the fading gain is estimated at both the relay and destination, separately. For CCE, we only consider the case when the fading gain is estimated at the destination. Based on these, the outage probability of AF relaying for DCE and CCE is derived for variable and fixed gains, respectively.

• We then derive the the general form of the bit error rate (BER) for high order modulations with DCE and CCE. We provide two kinds of closed-form approximations for DCE with different complexity and accuracy while we provide closed-form approximations for CCE with two kinds of amplification factors.

• More importantly, using the BER expressions of both DCE and CCE, the optimal values of pilot power under the total transmitting power constraint at the source and at the relay are obtained, separately. This is the case when the source, relay or destination are battery-limited moving nodes. Moreover, the optimal power allocation between the pilot power at the source, the pilot power at the relay, the data power at the source and the data power at the relay are obtained when their total transmitting power are fixed. This is the case when the source, relay and destination are fixed nodes that can be charged.

II. SYSTEM MODEL AND PILOT-AIDED ML ESTIMATION

Consider an AF cooperative system with one source, one destination and one relay. There is no direct link between the source and the destination. In the first time slot, the source transmits the signal to the relay such that the received signal at the relay can be expressed as

$$u(t) = \sqrt{E_d} \, h_1 \, s(t) + n_1(t) \tag{1}$$

where h_1 is the complex fading gain in the channel between the source and the relay, E_d is the transmitted signal energy per data symbol, $s(t)$ is the transmitted data symbol with the unit power such that $E\{|s(t)|^2\} = 1$, $E\{\cdot\}$ denotes the expectation operator, and n_1 is the complex additive white Gaussian noise (AWGN) in the channel between the source and the relay with noise power N_1.

In the second time slot, the received signal at the relay is amplified and forwarded such that the received signal at the destination is

$$y(t) = G \, h_2 \, u(t) + n_2(t) \tag{2}$$

where h_2 is the complex fading gain in the channel between the relay and the destination, n_2 is the complex AWGN in the channel between the relay and the destination with noise power N_2, and G is the amplification factor. Assume that all the links experience Rayleigh fading with $E\left\{|h_1|^2\right\} = \Omega_1$ and $E\left\{|h_2|^2\right\} = \Omega_2$. Assume that r is the path-loss exponent and that d_1 and d_2 are the distances between the source and the relay, the relay and the destination, respectively. Therefore, one has $\Omega_1 = L d_1^{-r}$ and $\Omega_2 = L d_2^{-r}$, where L is a constant that takes antenna gains and other power factors into account. We also assume that all nodes have similar transmitter/receiver settings such that L is the same for all hops.

Define the instantaneous signal-to-noise ratio (SNR) between source and relay, and between relay and destination as $\gamma_1 = E_d \, |h_1|^2 / N_1$ and $\gamma_2 = E_s \, |h_2|^2 / N_2$, respectively, and the average SNR as $\bar{\gamma}_1 = E_d \, \Omega_1 / N_1$ and $\bar{\gamma}_2 = E_s \, \Omega_2 / N_2$, respectively, where E_s is the transmitted energy per data symbol at the relay that is included in G. Therefore, the probability density functions (PDFs) of γ_1 and γ_2 are given by $f(\gamma_1) = \frac{1}{\bar{\gamma}_1} e^{-\frac{\gamma_1}{\bar{\gamma}_1}}$ and $f(\gamma_2) = \frac{1}{\bar{\gamma}_2} e^{-\frac{\gamma_2}{\bar{\gamma}_2}}$, respectively [10].

Consider the case when W_1 pilot symbols each with transmitted energy E_{w_1} are inserted before D data symbols at the source, giving a frame of $W_1 + D$ symbols. At the relay, in DCE, W_2 pilot symbols each with the transmitted energy E_{w_2} are inserted into the frame received from the source, while in CCE, the same pilot symbols W_1 from the source are amplified and forwarded to the destination with transmitted energy E_{w_2} such that no additional pilots are inserted at the relay. We still use the notation W_2 to denote the number of pilot symbols at the relay for CCE but $W_2 = W_1$ in this case.

Assume that n_{w_1} and n_{w_2} are the complex AWGN in the channel between source and relay, and the channel between relay and destination with noise power N_{w_1}, N_{w_2}, during the transmission of W_1, W_2 pilot symbols, respectively. Note that N_{w_1} and N_{w_2} can be the same as N_1 and N_2, respectively, but can also be different from N_1 and N_2, if one considers

the random interferences that occur in the pilot or data transmission periods separately. Also, assume block fading channels such that the fading gains remain the same during the whole frame.

Let P_T, P_1, P_2, P_d, P_s, P_{w_1} and P_{w_2} be the total power, the total power at the source, the total power at the relay, the total data power at the source, the total data power at the relay, the total pilot power at the source and the total pilot power at the relay, respectively. Therefore, one has $P_T = P_1 + P_2$, $P_1 = P_d + P_{w_1}$, $P_2 = P_s + P_{w_2}$, $P_d = D\ E_d$, $P_s = D\ E_s$, $P_{w_1} = W_1\ E_{w_1}$, $P_{w_2} = W_2\ E_{w_2}$ in both DCE and CCE. Let $H_1 = D+W_1$, $H_2 = D+W_2$ and $H = H_1+H_2$. Also, let P_1^*, P_2^*, P_d^*, P_s^*, $P_{w_1}^*$ and $P_{w_2}^*$ be the optimal total power at the source, the optimal total power at the relay, the optimal data power at the source, the optimal data power at the relay, the optimal pilot power at the source and the optimal pilot power at the relay, respectively. Note that in this paper we consider the optimal power for the whole frame in terms of P_d^*, P_s^*, $P_{w_1}^*$ and $P_{w_2}^*$, instead of the optimal power for one symbol as in [18], [23]. In this case, one can adjust either the number of symbols or the power of one symbol to achieve this under the total power constraints for specific application, which is more general and also more flexible than the optimal power for one symbol. Note also that this paper considers the case when the signal experiences block fading channel such that the channel gain keeps the same in one frame. Therefore, pilot symbols can be either interleaved with the data symbols or inserted as a preamble before the data symbols, as they do not need to sample the fading process. In fast fading channels, since the fading process is time-varying, these two schemes may be different and the interleaving rate will depend on the fading rate. In the following, we will introduce the amplification factor and ML estimation for both DCE and CCE.

A. DCE

In DCE, the amplification factor G is defined as [1]

$$\hat{G}_{var}^2 = \frac{E_s}{E_d \left|\hat{h}_1\right|^2 + N_1}. \qquad (3)$$

In this case, the relay and the destination estimate h_1 and h_2, separately. Let $h_1 = x_1 + iy_1$, where x_1, y_1 are independent and identically distributed random variables with zero mean and variance $\Omega_1/2$. Assume that $\hat{h}_1 = \hat{x}_1 + i\hat{y}_1$, where $\hat{h}_1$, $\hat{x}_1$, $\hat{y}_1$ are estimates of h_1, x_1, y_1 respectively. Using the pilot-symbol-aided ML estimation [22], one can have $\hat{x}_1 \sim \mathbb{N}(x_1, \frac{N_{w_1}}{2\ E_{w_1}W_1})$ and $\hat{y}_1 \sim \mathbb{N}(y_1, \frac{N_{w_1}}{2\ E_{w_1}W_1})$, where $\mathbb{N}\{\cdot, \cdot\}$ denotes the normal distribution. Therefore, one can get the PDF of $|\hat{h}_1|$ as

$$f_{|\hat{h}_1|}(x) = \frac{2xe^{-\frac{x^2 E_{w_1} W_1}{N_{w_1} + E_{w_1} \Omega_1 W_1}} E_{w_1} W_1}{N_{w_1} + E_{w_1} \Omega_1 W_1}, \quad x > 0. \qquad (4)$$

Similarly, one can get the PDF of $|\hat{h}_2|$ as

$$f_{|\hat{h}_2|}(x) = \frac{2xe^{-\frac{x^2 E_{w_2} W_2}{N_{w_2} + E_{w_2} \Omega_2 W_2}} E_{w_2} W_2}{N_{w_2} + E_{w_2} \Omega_2 W_2}, \quad x > 0. \qquad (5)$$

Define the estimated instantaneous SNR in the channel between the source and the relay, and that between the relay and the destination as $\hat{\gamma}_1 = E_d\ |\hat{h}_1|^2/N_1$ and $\hat{\gamma}_2 = E_s\ |\hat{h}_2|^2/N_2$, or $\hat{\gamma}_1 = \frac{P_d}{D}\ |\hat{h}_1|^2/N_1$ and $\hat{\gamma}_2 = \frac{P_s}{D}\ |\hat{h}_2|^2/N_2$, respectively. Therefore, one can calculate the estimated average SNR as $\bar{\hat{\gamma}}_1 = \bar{\gamma}_1 + \gamma_{\varepsilon_1}$ and $\bar{\hat{\gamma}}_2 = \bar{\gamma}_2 + \gamma_{\varepsilon_2}$, respectively, where γ_{ε_1} and γ_{ε_2} are defined as the statistics of the channel estimation errors between source and relay, and between relay and destination, respectively, with the values of $\gamma_{\varepsilon_1} = \frac{E_d N_{w_1}}{N_1 E_{w_1} W_1}$ and $\gamma_{\varepsilon_2} = \frac{E_s N_{w_2}}{N_2 E_{w_2} W_2}$. Thus, the PDF of $\hat{\gamma}_1$ and $\hat{\gamma}_2$ can be given by $f(\hat{\gamma}_1) = \frac{1}{\bar{\hat{\gamma}}_1}e^{-\frac{\hat{\gamma}_1}{\bar{\hat{\gamma}}_1}}$ and $f(\hat{\gamma}_2) = \frac{1}{\bar{\hat{\gamma}}_2}e^{-\frac{\hat{\gamma}_2}{\bar{\hat{\gamma}}_2}}$, respectively.

B. CCE

In CCE, the amplification factor G for the data symbols at the relay can be written as [3]

$$G_{d_{fix_1}}^2 = E\left[\frac{E_s}{E_d h_1^2 + N_1}\right] = \frac{E_s e^{\frac{N_1}{E_d \Omega_1}} \Gamma\left(0, \frac{N_1}{E_d \Omega_1}\right)}{E_d \Omega_1} \qquad (6)$$

or [24]

$$G_{d_{fix_2}}^2 = \frac{E_s}{E\left[E_d h_1^2 + N_1\right]} = \frac{E_s}{E_d \Omega_1 + N_1}. \qquad (7)$$

Similarly, the amplification factor for the pilot symbols at the relay is [3]

$$G_{w_{fix_1}}^2 = E\left[\frac{E_{w_2}}{E_{w_1} h_1^2 + N_{w_1}}\right] = \frac{E_{w_2} e^{\frac{N_{w_1}}{E_{w_1} \Omega_1}} \Gamma\left(0, \frac{N_{w_1}}{E_{w_1} \Omega_1}\right)}{E_{w_1} \Omega_1} \qquad (8)$$

or [24]

$$G_{w_{fix_2}}^2 = \frac{E_{w_2}}{E\left[E_{w_1} h_1^2 + N_{w_1}\right]} = \frac{E_{w_2}}{E_{w_1} \Omega_1 + N_{w_1}}. \qquad (9)$$

Instead of estimating h_1 and h_2 separately at the relay and at the destination as in DCE, we estimate the product of h_1 and h_2 at the destination in CCE. In this case, the relay uses a fixed gain which remains constant and no estimator is needed at the relay to simplify the structure of the relay. On the other hand, in DCE, extra energy is consumed to estimate the instantaneous CSI for $\hat{G}_{var}$, although DCE has a slightly better performance than CCE in some regions [4]. Define the instantaneous equivalent channel gain between the source and the destination as H. Then the received pilot symbol at destination can be written as

$$y = \sqrt{E_{w_1}}\ H\ G_{w_{fix_1}}\ s + n_w \qquad (10)$$

where $H = h_1\ h_2$ and $n_w = G_{w_{fix_1}}\ h_2\ n_{w_1} + n_{w_2}$. The PDF of $|H|$ is given as [25]

$$f_{|H|}(x) = \frac{4xK_0\left(2\sqrt{\frac{x^2}{\Omega_1\Omega_2}}\right)}{\Omega_1\Omega_2}, \quad x > 0. \qquad (11)$$

Define the estimated instantaneous equivalent channel gain between the source and the destination as $\hat{H}$. Also, n_w in (10) is non-Gaussian but is often approximated as Gaussian [16]. Thus, using the pilot-symbol-aided ML estimation [22]

and following the same process as in DCE, one can get the PDF of $|\hat{H}|$ as

$$f_{|\hat{H}|}(x) = \frac{4x K_0 \left(2\sqrt{\frac{x^2}{\Omega}}\right)}{\Omega}, \quad x > 0 \qquad (12)$$

where $\Omega = \Omega_1 \Omega_2 + \Omega_\varepsilon$, $\Omega_\varepsilon = \frac{N_{w_2} + G_{w_{fix_1}}^2 N_{w_1} \Omega_2}{E_{w_1} G_{w_{fix_1}}^2 W_1}$ can be considered as the variance of the channel estimation error. The PDF of $|\hat{H}|$ using $G_{w_{fix_2}}$ can be obtained in the same way.

III. BER AND OPTIMAL POWER ALLOCATION IN DCE

In this section, we first derive the outage probability and BER of AF using a variable gain in DCE and then study the optimal power allocation under the total transmitting power constraint. In the first subsection, we consider the case when the relay estimates h_1 and the destination has perfect knowledge of h_2. This is the case for mobile relays with limited complexity and power but fixed destination with enough power for accurate h_2. It serves as a benchmark for the case when both are estimated. In the second subsection, we consider the case when both the relay estimates h_1 and the destination estimates h_2, separately.

A. When h_1 is estimated at the relay

1) Outage probability and BER: The received signal at the destination can be written by omitting the time indexes as

$$y = \sqrt{E_d}\, h_1\, h_2\, \hat{G}_{var}\, s + \hat{G}_{var}\, h_2\, n_1 + n_2. \qquad (13)$$

Since $\hat{h}_1$ is the estimate of h_1 with $\hat{h}_1 = h_1 + \varepsilon_1$, where ε_1 is the channel estimation error, one has

$$y = \sqrt{E_d}\, (\hat{h}_1 - \varepsilon_1)\, h_2\, \hat{G}_{var}\, s + \hat{G}_{var}\, h_2\, n_1 + n_2. \qquad (14)$$

After simplification, one has

$$y = \sqrt{E_d}\, \hat{h}_1\, h_2\, \hat{G}_{var}\, s - \sqrt{E_d}\, \varepsilon_1\, h_2\, \hat{G}_{var}\, s + \hat{G}_{var}\, h_2\, n_1 + n_2. \qquad (15)$$

The end-to-end SNR can be derived from (15) as

$$\gamma_{end_1} = \frac{\gamma_2 \hat{\gamma}_1}{\gamma_2 + \hat{\gamma}_1 + 1 + \gamma_{\varepsilon_1}\, \gamma_2} \qquad (16)$$

where $E\{|\varepsilon_1|^2\} = \frac{N_{w_1}}{E_{w_1} W_1}$ and $E\{|s|^2\} = 1$ are assumed, and other symbols are defined as before. The value of ε_1 is considered as random disturbance, similar to noise. That is why ε_1 does not appear in (16) and only its statistics do. It is derived in Appendix A that the outage probability using the end-to-end SNR in (16) is

$$F_{\gamma_{end_1}}(\gamma_{th}) = 1 -$$

$$\frac{2 e^{-\frac{\gamma_{th}(\gamma_{\varepsilon_1} \bar{\gamma}_2 + \bar{\gamma}_1 + \bar{\gamma}_2)}{\bar{\gamma}_1 \bar{\gamma}_2}} K_1 \left(\frac{2}{\sqrt{\frac{\bar{\gamma}_2 \bar{\gamma}_1}{\gamma_{th}(\gamma_{\varepsilon_1}\, \gamma_{th} + \gamma_{th} + 1)}}}\right)}{\sqrt{\frac{\bar{\gamma}_2\, \bar{\gamma}_1}{\gamma_{th}(\gamma_{\varepsilon_1}\, \gamma_{th} + \gamma_{th} + 1)}}}, \qquad (17)$$

where $K_v(\cdot)$ is the vth order modified Bessel function of the second kind [26]. Using (17), the BER can be calculated as [27]

$$P_e = \frac{a}{2} \sqrt{\frac{b}{2\pi}} \int_0^\infty \frac{e^{-\frac{b}{2}x}}{\sqrt{x}} F_{\gamma_{end_1}}(x) dx \qquad (18)$$

where a and b are modulation-specific constants including $(a, b) = (1, 1)$ for BFSK, $(a, b) = (1, 2)$ for BPSK and $(a, b) = (2\frac{M-1}{M}, \frac{6}{M^2-1})$ for M-PAM. Also, the BER expression in (18) is a good approximation to the BER of some higher order modulations, such as $(a, b) = (2, 2\, sin^2(\pi/M))$ for M-PSK.

The BER in (18) can be approximated in two ways. First, one can approximate the BER as

$$P_e \approx \frac{1}{2} a \left(1 - \frac{\sqrt{b}}{\sqrt{b + 2\beta_2}}\right) \qquad (19)$$

where $\beta_2 = \frac{\bar{\gamma}_1 + \bar{\gamma}_2 \gamma_{\varepsilon_1} + \bar{\gamma}_2}{\hat{\gamma}_1 \bar{\gamma}_2}$.
Proof: See Appendix B.
Second, one can get the approximate BER as (20), where $\beta_1 = \frac{2\sqrt{\gamma_{\varepsilon_1} + 1}}{\sqrt{\hat{\gamma}_1 \bar{\gamma}_2}}$, $\kappa_\nu(\cdot)$ is the complete elliptic integral of the νth kind defined in [26] with $\kappa_1(k) = \int_0^{\pi/2} \frac{dx}{\sqrt{1-k\sin^2(x)}}$ and $\kappa_2(k) = \int_0^{\pi/2} \sqrt{1 - k\sin^2(x)}\, dx$.
Proof: See Appendix C.

2) Optimal power allocation: Since we consider the case when the relay estimates h_1 and the destination has perfect knowledge of h_2, we only derive the optimal power allocation between P_d and P_{w_1} under the fixed total power P_1 at the source. Since (19) is simpler than both (18) and (20), we use (19) to derive the optimal allocation. One can observe that minimizing (19) is equivalent to minimizing β_2. Inserting $E_d = \frac{P_d}{D}$, $E_{w_1} = \frac{P_{w_1}}{W_1}$ and $P_d = P_1 - P_{w_1}$ into β_2, one can get

$$\beta_2 = \frac{D P_{w_1} N_1}{(P_1 - P_{w_1})(P_{w_1}\Omega_1 + N_{w_1})} + \frac{N_2}{E_s \Omega_2} + \frac{N_{w_1}}{P_{w_1}\Omega_1 + N_{w_1}}. \qquad (21)$$

Differentiating (21) with respect to P_{w_1}, equating it to zero and solving the equation, the optimal value of P_{w_1} can be found as

$$P_{w_1}^* = \frac{\mu_1 - P_1 N_{w_1}\Omega_1}{D N_1 \Omega_1 - N_{w_1}\Omega_1} \qquad (22)$$

where $\mu_1 = (-D^2 P_1 N_1^2 N_{w_1}\Omega_1 + D P_1^2 N_1 N_{w_1}\Omega_1^2 + D P_1 N_1 N_{w_1}^2 \Omega_1)^{1/2}$. Then, by using $P_{w_1}^*$ of (22), the optimal value of P_d can be found as $P_d^* = P_1 - P_{w_1}^*$. One can see from (22) that the optimal pilot power at the source increases when Ω_1 increases, or when the distance between the source and the relay decreases, as $\Omega_1 = L d_1^{-r}$.

B. When both h_1 and h_2 are estimated at the relay and at the destination, separately

1) Outage probability and BER: In this case, the received signal at destination can be written as

$$y = \sqrt{E_d}\, h_1\, h_2\, \hat{G}_{var}\, s + \hat{G}_{var}\, h_2\, n_1 + n_2. \qquad (23)$$

$$P_e \approx \frac{1}{2}a\sqrt{b}\left(\frac{\sqrt{\beta_1}\left((b+2(\beta_1+\beta_2))\kappa_1\left(-\frac{b-2\beta_1+2\beta_2}{4\beta_1}\right)-2(b+2\beta_2)\kappa_2\left(-\frac{b-2\beta_1+2\beta_2}{4\beta_1}\right)\right)}{(b-2\beta_1+2\beta_2)(b+2(\beta_1+\beta_2))}+\frac{1}{\sqrt{b}}\right) \tag{20}$$

Let $\hat{h}_1$, $\hat{h}_2$ be the estimates of h_1, h_2, respectively, with $\hat{h}_1 = \varepsilon_1 + h_1$ and $\hat{h}_2 = \varepsilon_2 + h_2$ where ε_1 and ε_2 are the channel estimation errors. Thus,

$$y = \sqrt{E_d}\left(\hat{h}_1 - \varepsilon_1\right)\left(\hat{h}_2 - \varepsilon_2\right)\hat{G}_{var}\,s + \hat{G}_{var}\left(\hat{h}_2 - \varepsilon_2\right)n_1 + n_2. \tag{24}$$

The end-to-end SNR in this case can be written as

$$\gamma_{end_2} = \frac{\hat{\gamma}_2\hat{\gamma}_1}{\hat{\gamma}_2\gamma_{\varepsilon_1}+\hat{\gamma}_1\gamma_{\varepsilon_2}+\gamma_{\varepsilon_1}\,\gamma_{\varepsilon_2}+\hat{\gamma}_2+\hat{\gamma}_1+1+\gamma_{\varepsilon_2}} \tag{25}$$

where $E\{|s|^2\} = 1$, $E\{|\varepsilon_1|^2\} = \frac{N_{w_1}}{E_{w_1}W_1}$, $E\{|\varepsilon_2|^2\} = \frac{N_{w_2}}{E_{w_2}W_2}$ and other symbols are defined as before. It is derived in Appendix D that the outage probability of the end-to-end SNR in (25) is

$$F_{\gamma_{end_2}}(\gamma_{th}) = 1 - 2e^{-\frac{\gamma_{th}(\gamma_{\varepsilon_1}\bar{\hat{\gamma}}_2+\gamma_{\varepsilon_2}\bar{\hat{\gamma}}_1+\bar{\hat{\gamma}}_1+\bar{\hat{\gamma}}_2)}{\bar{\hat{\gamma}}_1\bar{\hat{\gamma}}_2}}$$

$$\times \frac{K_1\left(\sqrt{\frac{2}{\frac{\bar{\hat{\gamma}}_1\bar{\hat{\gamma}}_2}{\gamma_{th}(\gamma_{\varepsilon_1}\gamma_{th}+\gamma_{th}+(\gamma_{\varepsilon_1}+1)\gamma_{\varepsilon_2}(\gamma_{th}+1)+1)}}}\right)}{\sqrt{\frac{\bar{\hat{\gamma}}_1\bar{\hat{\gamma}}_2}{\gamma_{th}((\gamma_{\varepsilon_1}+1)\gamma_{\varepsilon_2}(\gamma_{th}+1)+\gamma_{\varepsilon_1}\gamma_{th}+\gamma_{th}+1)}}}. \tag{26}$$

Similarly, the BER is given by

$$P_e = \frac{a}{2}\sqrt{\frac{b}{2\pi}}\int_0^\infty \frac{e^{-\frac{b}{2}x}}{\sqrt{x}}F_{\gamma_{end_2}}(x)dx. \tag{27}$$

Using the same approximations as before, the BER in (27) can be approximated as

$$P_e \approx \frac{1}{2}a\left(1 - \frac{\sqrt{b}}{\sqrt{b+2\beta_4}}\right) \tag{28}$$

or (29), where $\beta_3 = \frac{2\sqrt{(\gamma_{\varepsilon_1}+1)(\gamma_{\varepsilon_2}+1)}}{\sqrt{\bar{\hat{\gamma}}_1\bar{\hat{\gamma}}_2}}$ and $\beta_4 = \frac{\bar{\hat{\gamma}}_1\gamma_{\varepsilon_2}+\bar{\hat{\gamma}}_1+\bar{\hat{\gamma}}_2\gamma_{\varepsilon_1}+\bar{\hat{\gamma}}_2}{\bar{\hat{\gamma}}_1\bar{\hat{\gamma}}_2}$.

2) Optimal power allocation: In the first part of this subsection, we consider the optimal allocation between P_d and P_{w_1} under fixed P_1, and the optimal allocation between P_s and P_{w_2} under fixed P_2, separately. In the second part, we consider the optimal allocation between P_d, P_s, P_{w_1}, P_{w_2} under the fixed total power P_T. Similarly, we use β_4 in (28) to derive the optimal power allocation below.

Firstly, by inserting $E_d = \frac{P_d}{D}$, $E_s = \frac{P_s}{D}$, $E_{w_1} = \frac{P_{w_1}}{W_1}$, $E_{w_2} = \frac{P_{w_2}}{W_2}$, $P_d = P_1 - P_{w_1}$ and $P_s = P_2 - P_{w_2}$ into β_4, one can get

$$\beta_4 = \frac{DP_{w_1}N_1 + N_{w_1}(P_1 - P_{w_1})}{N_{w_1}(P_1 - P_{w_1}) + P_{w_1}\Omega_1(P_1 - P_{w_1})} + \frac{DP_{w_2}N_2 + N_{w_2}(P_2 - P_{w_2})}{N_{w_2}(P_2 - P_{w_2}) + P_{w_2}\Omega_2(P_2 - P_{w_2})}. \tag{30}$$

Differentiating (30) with respect to P_{w_1}, P_{w_2} and equating them to zero, respectively, the optimal values of P_{w_1} and P_{w_2}

can be found as

$$P_{w_1}^* = \frac{\mu_1 - P_1 N_{w_1}\Omega_1}{DN_1\Omega_1 - N_{w_1}\Omega_1} \tag{31}$$

and

$$P_{w_2}^* = \frac{\mu_2 - P_2 N_{w_2}\Omega_2}{DN_2\Omega_2 - N_{w_2}\Omega_2} \tag{32}$$

respectively, where $\mu_2 = (-D^2 P_2 N_2^2 N_{w_2}\Omega_2 + DP_2^2 N_2 N_{w_2}\Omega_2^2 + DP_2 N_2 N_{w_2}^2 \Omega_2)^{1/2}$. Then, by using $P_{w_1}^*$ of (31) and $P_{w_2}^*$ of (32), the optimal values of P_d and P_s can be found as $P_d^* = P_1 - P_{w_1}^*$ and $P_s^* = P_2 - P_{w_2}^*$, respectively.

Secondly, inserting $P_{w_1}^*$, $P_{w_2}^*$, P_d^*, P_s^* and $P_2 = P_T - P_1$ into β_4 in (30), differentiating it with respect to P_1, equating it to zero and solving the equation, one can get

$$\frac{\alpha_{10}^2(\alpha_4(\alpha_3 - 2N_{w_1}\Omega_1\alpha_4) - \alpha_2\alpha_3)}{\alpha_1\alpha_2^2\alpha_4} +$$
$$\frac{\alpha_7^2\left(2\Omega_2\alpha_6^2(DN_2\alpha_8 + N_{w_2}\alpha_5) + \alpha_9(\alpha_5(\alpha_6 - \alpha_8) + \alpha_6\alpha_8)\right)}{\alpha_5^2\alpha_6\alpha_8^2}$$
$$+ \frac{\alpha_{10}^2(\alpha_3 - 2DN_1\Omega_1\alpha_4)}{\alpha_1^2\alpha_2} = 0 \tag{33}$$

where $\alpha_1 = \alpha_4 - DP_1 N_1\Omega_1$, $\alpha_2 = DN_1 N_{w_1} - P_1 N_{w_1}\Omega_1 - N_{w_1}^2 + \alpha_4$, $\alpha_3 = DP_1 N_1 N_{w_1}\Omega_1^2 - DN_1 N_{w_1}\Omega_1(DN_1 - P_1\Omega_1 - N_{w_1})$, $\alpha_4 = [-DP_1 N_1 N_{w_1}\Omega_1(DN_1 - P_1\Omega_1 - N_{w_1})]^{1/2}$, $\alpha_5 = \alpha_6 - DN_2\Omega_2(P_T - P_1)$, $\alpha_6 = [-DN_2 N_{w_2}\Omega_2(P_T - P_1)(DN_2 - \Omega_2(P_T - P_1) - N_{w_2})]^{1/2}$, $\alpha_7 = N_{w_2} - DN_2$, $\alpha_8 = DN_2 N_{w_2} - N_{w_2}\Omega_2(P_T - P_1) - N_{w_2}^2 + \alpha_6$, $\alpha_9 = DN_2 N_{w_2}\Omega_2(DN_2 - \Omega_2(P_T - P_1) - N_{w_2}) - DN_2 N_{w_2}\Omega_2^2(P_T - P_1)$ and $\alpha_{10} = N_{w_1} - DN_1$. Note that (33) does not lead to a closed-form expression for the optimal value of P_1^* but can be calculated numerically by using commonly adopted mathematical software packages, such as MATLAB, MATHEMATICA and MAPLE. With the optimal value of P_1^* obtained from (33), one can easily calculate the optimal value of P_2^* and the following optimal values of P_d^*, P_s^*, $P_{w_1}^*$ and $P_{w_2}^*$ under the fixed total power P_T. Note that the optimal value of P_1^* obtained from (33) is the exact optimal value for the total power at the source. In the following, we give a simpler approximate closed-form value for P_1^* under high SNR conditions. When the SNR is high, β_4 in (30) can be approximated as

$$\beta_5 \approx \frac{DP_{w_1}N_1 + N_{w_1}(P_1 - P_{w_1})}{P_{w_1}\Omega_1(P_1 - P_{w_1})} + \frac{DP_{w_2}N_2 + N_{w_2}(P_2 - P_{w_2})}{P_{w_2}\Omega_2(P_2 - P_{w_2})}. \tag{34}$$

Differentiating (34) with respect to P_{w_1}, P_{w_2} and equating them to zero, respectively, the optimal values of P_{w_1} and P_{w_2} can also be found as

$$P_{w_1}^* = \frac{P_1\mu_5}{\mu_3} \tag{35}$$

$$P_e \approx \frac{1}{2} a \sqrt{b} \left(\frac{\sqrt{\beta_3} \left((b + 2(\beta_3 + \beta_4)) \kappa_1 \left(-\frac{b - 2\beta_3 + 2\beta_4}{4\beta_3} \right) - 2(b + 2\beta_4) \kappa_2 \left(-\frac{b - 2\beta_3 + 2\beta_4}{4\beta_3} \right) \right)}{(b - 2\beta_3 + 2\beta_4)(b + 2(\beta_3 + \beta_4))} + \frac{1}{\sqrt{b}} \right) \tag{29}$$

and

$$P_{w_2}^* = \frac{P_2 \mu_6}{\mu_4} \tag{36}$$

respectively, where $\mu_3 = DN_1 - N_{w_1}, \mu_4 = DN_2 - P_{w_2}, \mu_5 = \sqrt{DN_1 N_{w_1}} - N_{w_1}, \mu_6 = \sqrt{DN_2 N_{w_2}} - N_{w_2}$. By using $P_{w_1}^*$ in (35) and $P_{w_2}^*$ in (36), the optimal values of P_d and P_s can be found as $P_d^* = P_1 - P_{w_1}^*$ and $P_s^* = P_2 - P_{w_2}^*$, respectively. One can see from (35) and (36) that the optimal pilot powers at the source and at the relay increase with the increases of P_1 and P_2, respectively. Then, by inserting $P_{w_1}^*, P_{w_2}^*, P_d^*, P_s^*$ and $P_2 = P_T - P_1$ into β_4 in (30) and differentiating it with respect to P_1, and equating it to zero, one can get

$$\sqrt{\frac{\Omega_1 \mu_3 \mu_5 (\mu_4 - \mu_6)(DN_1 \mu_5 + N_{w_1}(\mu_3 - \mu_5))}{\Omega_2 \mu_4 \mu_6 (\mu_3 - \mu_5)(DN_2 \mu_6 + N_{w_2}(\mu_4 - \mu_6))}} = \frac{P_1 \Omega_1 \mu_5 + N_{w_1} \mu_3}{(P_T - P_1) \Omega_2 \mu_6 + N_{w_2} \mu_4}. \tag{37}$$

Letting $\mu_7 = \sqrt{\frac{\Omega_1 \mu_3 \mu_5 (\mu_4 - \mu_6)(DN_1 \mu_5 + N_{w_1}(\mu_3 - \mu_5))}{\Omega_2 \mu_4 \mu_6 (\mu_3 - \mu_5)(DN_2 \mu_6 + N_{w_2}(\mu_4 - \mu_6))}}$, one can get

$$P_1^* = \frac{P_T \Omega_2 \mu_6 \mu_7 - N_{w_1} \mu_3 + N_{w_2} \mu_4 \mu_7}{\Omega_1 \mu_5 + \Omega_2 \mu_6 \mu_7}. \tag{38}$$

With the value of P_1^* obtained in (38), one can easily calculate the value of P_2^* and the following optimal values of $P_d^*, P_s^*, P_{w_1}^*$ and $P_{w_2}^*$ under the fixed total power P_T. Note that from our simulations, it is found that the values of $P_{w_1}^*$ in (35) and $P_{w_2}^*$ in (36) are nearly the same as the values of $P_{w_1}^*$ in (31) and $P_{w_2}^*$ in (32), respectively. Thus (35) and (36) are very good approximations. Also, the optimal value of P_1^* obtained from (38) is nearly the same as the value obtained in equation (33), but (38) gives a closed-form expression of P_1^*, which is preferable in some applications.

IV. BER AND OPTIMAL PILOT POWER ALLOCATION IN CCE

In this section, we first derive the outage probability and BER of AF using a fixed gain in CCE, and then derive the optimal power under the total transmit power constraints. In the first subsection, we use $G_{d_{fix_1}}$ and $G_{w_{fix_1}}$, while in the second subsection, we use $G_{d_{fix_2}}$ and $G_{w_{fix_2}}$.

A. Using $G_{d_{fix_1}}$ and $G_{w_{fix_1}}$

1) Outage probability and BER: In this case, the received signal at the destination is

$$y = \sqrt{E_d} \, h_1 \, h_2 \, G_{d_{fix_1}} \, s + G_{d_{fix_1}} \, h_2 \, n_1 + n_2. \tag{39}$$

Assuming $H = h_1 \, h_2$ and $n = G_{d_{fix_1}} \, h_2 \, n_1 + n_2$, (39) becomes

$$y = \sqrt{E_d} \, H \, G_{d_{fix_1}} \, s + n. \tag{40}$$

Let $\hat{H}$ be the estimate of H, and $\hat{H} = H + \varepsilon$, where ε denotes the channel estimation error. One has

$$y = \sqrt{E_d} \, \hat{H} \, G_{d_{fix_1}} \, s - \sqrt{E_d} \, \varepsilon \, G_{d_{fix_1}} \, s + n. \tag{41}$$

The end-to-end SNR can be derived from (41) as

$$\gamma_{fix} = \frac{E_d \, \hat{H}^2 \, G_{d_{fix_1}}^2}{E_d \, \Omega_\varepsilon \, G_{d_{fix_1}}^2 + N} \tag{42}$$

where $N = G_{d_{fix_1}}^2 \, N_1 \Omega_2 + N_2$ and $E\{|s|^2\} = 1$. It is derived in Appendix E that the outage probability of the end-to-end SNR in (42) can be written as

$$F_{\gamma_{fix}}(\gamma_{th}) = 1 - 2 \sqrt{\frac{\gamma_{th}(E_d \Omega_\varepsilon G_{d_{fix_1}}^2 + N)}{E_d G_{d_{fix_1}}^2 \Omega}}$$
$$\times K_1 \left(2 \sqrt{\frac{\gamma_{th}(E_d \Omega_\varepsilon G_{d_{fix_1}}^2 + N)}{E_d G_{d_{fix_1}}^2 \Omega}} \right). \tag{43}$$

Using γ_{fix} in (42), the BER is derived as

$$P_e = \int_0^\infty a Q \left(\sqrt{b \frac{E_d \, \hat{H}^2 \, G_{d_{fix_1}}^2}{E_d \, \Omega_\varepsilon \, G_{d_{fix_1}}^2 + N}} \right) f_{\hat{H}}(\hat{H}) d\hat{H}. \tag{44}$$

One can use the PDF of $\hat{H}$ in (12) with [26, (6.62)] to solve the integral as

$$P_e = \frac{a G_{2,3}^{2,2} \left(\frac{2(E_d \Omega_\varepsilon G_{d_{fix_1}}^2 + N)}{b E_d G_{d_{fix_1}}^2 \Omega} \Big| \begin{matrix} \frac{1}{2}, 1 \\ 1, 1, 0 \end{matrix} \right)}{2\sqrt{\pi}} \tag{45}$$

where a, b are defined as in (18) and $G_{2,3}^{2,2}(\cdot)$ denotes the Meijer's $G-$function [26]. Using the approximation $\Gamma[0, x] \approx \frac{-e^{-x}}{-x}$ [26] in (6) and (8), one can have $G_{d_{fix_1}}^2 \approx \frac{E_s}{N_1}$ and $G_{w_{fix_1}}^2 \approx \frac{E_{w_2}}{N_{w_1}}$. Therefore, the BER in (45) can be approximated as (46).

2) Optimal power allocation: Denoting β_6 as

$$\beta_6 = [2(E_d E_s N_{w_1}(N_{w_2} + E_{w_2}\Omega_2) + E_{w_1} E_{w_2} N_1$$
$$(N_2 + E_s \Omega_2) W_1)] / [b E_d E_s(N_{w_1}(N_{w_2} + E_{w_2}\Omega_2) \tag{47}$$
$$+ E_{w_1} E_{w_2} \Omega_1 \Omega_2 W_1)],$$

one can observe that minimizing P_e in (46) is equivalent to minimizing β_6. However, β_6 in (47) is a complicated function that does not lead to any closed-form expressions for the optimal power allocation. Therefore, we simplify the equations for high SNR as

$$\beta_6 \approx \frac{2E_d N_{w_1} + 2E_{w_1} N_1 W_1}{b E_d E_{w_1} \Omega_1 W_1 + b E_d N_{w_1}}. \tag{48}$$

Note that the high SNR approximation is used only to derive the closed-form solutions of the power allocation but the derived optimal values can be used for all SNRs and BERs,

$$P_e \approx \frac{aG_{2,3}^{2,2}\left(\frac{2(E_dE_sN_{w_1}(N_{w_2}+E_{w_2}\Omega_2)+E_{w_1}E_{w_2}N_1(N_2+E_s\Omega_2)W_1)}{bE_dE_s(N_{w_1}(N_{w_2}+E_{w_2}\Omega_2)+E_{w_1}E_{w_2}\Omega_1\Omega_2W_1)}\Big|\ \begin{matrix}\frac{1}{2},1\\1,1,0\end{matrix}\right)}{2\sqrt{\pi}}. \tag{46}$$

which will be justified in Section V. By inserting $E_d = \frac{P_d}{D}$, $E_{w_1} = \frac{P_{w_1}}{W_1}$ and $P_d = P_1 - P_{w_1}$ into β_6 in (48) and differentiating it with respect to P_{w_1}, then equating it to zero, one can get the optimal value of P_{w_1} as

$$P_{w_1}^* = \frac{\mu_1 - P_1N_{w_1}\Omega_1}{DN_1\Omega_1 - N_{w_1}\Omega_1}. \tag{49}$$

Then, the optimal value of P_d can be found as $P_d^* = P_1 - P_{w_1}^*$. One can see that (48) does not include E_s and E_{w_2} due to high SNR approximation. Therefore, we use β_6 of (47) to get the optimal values of P_s and P_{w_2}. By inserting $E_s = \frac{P_s}{D}$, $E_{w_2} = \frac{P_{w_2}}{W_2}$ and $P_s = P_2 - P_{w_2}$ into β_6 of (47) and differentiating it with respect to P_{w_2}, then equating it to zero, one can get the optimal value of P_{w_2} as

$$P_{w_2}^* = [\mu_8 + P_2N_{w_1}N_{w_2}\Omega_2W_1(DN_1 - P_d\Omega_1)]/[D^2N_1N_2$$
$$\Omega_2(P_{w_1}^*\Omega_1 + N_{w_1}) + N_{w_1}N_{w_2}\Omega_2W_1(DN_1 - P_d\Omega_1)] \tag{50}$$

where $\mu_8 = [D^2P_2N_1N_2N_{w_1}N_{w_2}\Omega_2W_1((P_{w_1}^*\Omega_1 + N_{w_1})(-D^2N_1N_2 + D(-P_2)N_1\Omega_2 + P_2P_d\Omega_1\Omega_2) + N_{w_1}N_{w_2}W_1(P_d\Omega_1 - DN_1))]^{1/2}$. Then, the optimal value of P_s can be found as $P_s^* = P_2 - P_{w_2}^*$. In this case, the optimal power allocation between P_d, P_s, P_{w_1}, P_{w_2} under the fixed total power P_T can be obtained by first inserting $P_{w_1}^*$, $P_{w_2}^*$, P_d^*, P_s^* and $P_2 = P_T - P_1$ into β_6 in (47) and differentiating it with respect to P_1, then equating it to zero. However, the results are not presented here since it is very complicated and do not provide much insight to the performance analysis, although it can be easily extracted using the well-known mathematical software packages. We will provide the optimal power allocation between P_d, P_s, P_{w_1}, P_{w_2} under fixed P_T for the case when $G_{d_{fix_2}}$ in (7) and $G_{w_{fix_2}}$ in (9) are used in the next subsection.

B. Using $G_{d_{fix_2}}$ and $G_{w_{fix_2}}$

1) Outage probability and BER: In this case, using $G_{d_{fix_2}}$ in (7) and $G_{w_{fix_2}}$ in (9), the outage probability can be easily obtained by replacing $G_{d_{fix_1}}$ and $G_{w_{fix_1}}$ in (43) with $G_{d_{fix_2}}$ and $G_{w_{fix_2}}$, respectively. Also, the BER expression P_e in (44) can be solved as (51), where a, b are defined as in (18). Using the approximations of $G_{d_{fix_2}}^2 \approx \frac{E_s}{E_d\Omega_1}$ and $G_{w_{fix_2}}^2 \approx \frac{E_{w_2}}{E_{w_1}\Omega_1}$ in high SNR, the BER in (51) can be approximated as (52).

2) Optimal power allocation: Denoting β_7 as

$$\beta_7 = [2(E_{w_1}E_{w_2}W_1(E_dN_2\Omega_1 + E_sN_1\Omega_2) + E_dE_s$$
$$(E_{w_1}N_{w_2}\Omega_1 + E_{w_2}N_{w_1}\Omega_2))]/[bE_dE_s(E_{w_1}\Omega_1(E_{w_2}\Omega_2W_1$$
$$+ N_{w_2}) + E_{w_2}N_{w_1}\Omega_2)]. \tag{53}$$

One can observe that minimizing P_e in (52) is equivalent to minimizing β_7. However, β_7 in (53) is a complicated function that does not lead to any closed-form expressions for optimal

power allocation. Therefore, we simplify β_7 for high SNR as

$$\beta_7 \approx [2E_dE_{w_1}E_{w_2}N_2\Omega_1W_1 + 2E_dE_{w_1}E_sN_{w_2}\Omega_1+$$
$$2E_dE_{w_2}E_sN_{w_1}\Omega_2 + 2E_{w_1}E_{w_2}E_sN_1\Omega_2W_1]/[bE_dE_{w_1}E_{w_2}$$
$$E_s\Omega_1\Omega_2W_1 + bE_dE_{w_2}E_sN_{w_1}\Omega_2]. \tag{54}$$

Firstly, by inserting $E_d = \frac{P_d}{D}$, $E_s = \frac{P_s}{D}$, $E_{w_1} = \frac{P_{w_1}}{W_1}$, $E_{w_2} = \frac{P_{w_2}}{W_2}$, $P_s = P_2 - P_{w_2}$ and $P_d = P_1 - P_{w_1}$ into β_7 in (54) and differentiating it with respect to P_{w_1} and P_{w_2}, then equating them to zero, respectively, one can get the optimal value of P_{w_2} as

$$P_{w_2}^* = \frac{P_2\sqrt{N_2DN_{w_2}} - P_2N_{w_2}}{DN_2 - N_{w_2}} \tag{55}$$

and the optimal value of P_{w_1} as

$$P_{w_1}^* =$$
$$\frac{\mu_9 + P_1N_{w_1}\Omega_1(DP_{w_2}^*N_2 + P_s(N_{w_2} - P_{w_2}^*\Omega_2))}{\Omega_1(DP_{w_2}^*(P_sN_1\Omega_2 + N_2N_{w_1}) + P_sN_{w_1}(N_{w_2} - P_{w_2}^*\Omega_2))} \tag{56}$$

where $\mu_9 = (-DP_1P_{w_2}^*P_sN_1N_{w_1}\Omega_1\Omega_2(DP_{w_2}^*(N_2(P_1\Omega_1 + N_{w_1}) + P_sN_1\Omega_2) + P_s(P_1\Omega_1 + N_{w_1})(N_{w_2} - P_{w_2}^*\Omega_2)))^{1/2}$. Then, by using $P_{w_1}^*$ in (56) and $P_{w_2}^*$ in (55), the optimal values of P_d and P_s can be found as $P_d^* = P_1 - P_{w_1}^*$ and $P_s^* = P_2 - P_{w_2}^*$, respectively.

Secondly, in order to get the optimal power allocation between P_d, P_s, P_{w_1}, P_{w_2} under fixed P_T, $P_{w_1}^*$ in (56) and $P_{w_2}^*$ in (55) must be approximated to obtain simpler forms. Following the same process as that in Section III.B, β_7 in (54) can be approximated as

$$\beta_8 \approx$$
$$\frac{2\left(DP_{w_1}\left(\frac{N_1}{P_1-P_{w_1}} + \frac{N_2\Omega_1}{P_2\Omega_2-P_{w_2}\Omega_2}\right) + \frac{P_{w_1}N_{w_2}\Omega_1}{P_{w_2}\Omega_2} + N_{w_1}\right)}{b(P_{w_1}\Omega_1 + N_{w_1})}. \tag{57}$$

Differentiating β_8 in (57) with respect to P_{w_1}, P_{w_2} and equating them to zero, respectively, the approximate optimal values of P_{w_1} and P_{w_2} can be found as

$$P_{w_1}^* = \frac{P_1\mu_5}{\mu_3} \tag{58}$$

and

$$P_{w_2}^* = \frac{P_2\mu_6}{\mu_4} \tag{59}$$

respectively. One can see that $P_{w_1}^*$ and $P_{w_2}^*$ in (58) and (59) are the same as the optimal values obtained in Section III.B for DCE. By using $P_{w_1}^*$ in (58) and $P_{w_2}^*$ in (59), the approximate optimal values of P_d and P_s can be found as $P_d^* = P_1 - P_{w_1}^*$ and $P_s^* = P_2 - P_{w_2}^*$ respectively. Then, by inserting those approximate $P_{w_1}^*$, $P_{w_2}^*$, P_d^*, P_s^* and $P_2 = P_T - P_1$ into β_8 and differentiating it with respect to P_1, then equating it to zero, one can get

$$P_1^* = \frac{\sqrt{P_T^2\mu_{11}\mu_{12} - \mu_{10}\mu_{11} + \mu_{10}\mu_{12}} - P_T\mu_{12}}{\mu_{11} - \mu_{12}} \tag{60}$$

$$P_e = \frac{aG_{2,3}^{2,2}\left(\frac{2E_dE_s(E_{w_1}N_{w_2}\Omega_1+N_{w_1}(N_{w_2}+E_{w_2}\Omega_2))+2E_{w_1}E_{w_2}(E_dN_2\Omega_1+N_1(N_2+E_s\Omega_2))W_1}{bE_dE_s(N_{w_1}(N_{w_2}+E_{w_2}\Omega_2)+E_{w_1}\Omega_1(N_{w_2}+E_{w_2}\Omega_2W_1))}\Big|\begin{array}{c}\frac{1}{2},1\\1,1,0\end{array}\right)}{2\sqrt{\pi}} \tag{51}$$

$$P_e = \frac{aG_{2,3}^{2,2}\left(\frac{2(E_dE_s(E_{w_1}N_{w_2}\Omega_1+E_{w_2}N_{w_1}\Omega_2)+E_{w_1}E_{w_2}(E_dN_2\Omega_1+E_sN_1\Omega_2)W_1)}{bE_dE_s(E_{w_2}N_{w_1}\Omega_2+E_{w_1}\Omega_1(N_{w_2}+E_{w_2}\Omega_2W_1))}\Big|\begin{array}{c}\frac{1}{2},1\\1,1,0\end{array}\right)}{2\sqrt{\pi}}. \tag{52}$$

where $\mu_{10} = P_TN_{w_1}\mu_3\mu_4(\mu_3-\mu_5)(DN_2\mu_6+N_{w_2}(\mu_4-\mu_6))$, $\mu_{11} = \Omega_1\mu_4\mu_5(\mu_3-\mu_5)(DN_2\mu_6+N_{w_2}(\mu_4-\mu_6))$ and $\mu_{12} = \Omega_2\mu_3\mu_6(\mu_4-\mu_6)(DN_1\mu_5+N_{w_1}(\mu_3-\mu_5))$. With the value of P_1^* obtained in (60), one can easily calculate the value of P_2^* and the following optimal values of P_d^*, P_s^*, $P_{w_1}^*$ and $P_{w_2}^*$ under the fixed total power P_T. Similarly, these approximate optimal values obtained here are nearly the same with the exact values from our simulations, as will be shown later.

V. NUMERICAL RESULTS AND DISCUSSION

In this section, numerical results are presented to illustrate and verify our theoretical analysis. In the first subsection, the BER expressions of AF using a variable gain in DCE and using two types of fixed gain in CCE are examined. In the simulation, 10^6 Monte-Carlo simulation runs are used. Each run has a different channel realization but the same bit. There is no iteration. In the second subsection, the BER performances with optimal power values are compared with the conventional system without optimal power allocation. We use $(a, b) = (1, 2)$ for BPSK, $(a, b) = (1.5, 0.4)$ for 4-PAM and $(a, b) = (2, 1)$ for the approximation of QPSK. Also, we use $L = 1$, the path-loss exponent $r = 3$, $W_1 = 5$, $W_2 = 5$ and $D = 45$ in the examples below. Note that the total pilot power and the total data power, not the individual symbol powers, are optimized in this paper. As a result, one can either fix the individual symbol powers and optimize the symbol numbers, or fix the symbol numbers and optimize the individual symbol powers, or both. In the examples, we fix the symbol numbers and optimize the individual symbol powers. Other values of W_1, W_2 and D or other methods of optimization can be examined in a similar way. They have the same effects as it is the total power that determines the system performance and that is optimized. Denote the BER expressions in (18), (27), (45) or (51) as "Exact", the BER expressions in (19), (28), (46) or (52) as "Approximation-1" and BER expressions in (20) or (29) as "Approximation-2". Exact BER expressions in (18) and (27) in the form of one-dimensional integral are calculated numerically by using the "NIntegrate" method in MATHEMATICA software package while other BER expressions in closed-form are calculated directly.

A. Validation of BER Expressions

Fig. 1 - Fig. 3 show the BERs vs. $\bar{\gamma}_1$, where we set $d_1 = 1$, $d_2 = 1$, $N_1 = 1$, $N_2 = 1$, $N_{w_1} = 1$, $N_{w_2} = 1$, $\gamma_{\varepsilon_1} = -10$ dB and $\bar{\gamma}_1 = 2\bar{\gamma}_2$. One can see from Fig. 1 - Fig. 3 that BPSK gives the best BER performance while 4-PAM gives the worst

BER performance. But QPSK and 4-PAM can transmit twice the data rate in a given bandwidth compared to BPSK. Thus it is a tradeoff between reliability and rate.

Fig. 1 (a) compares the BERs obtained by simulation, "Exact" in (18), "Approximation-1" in (19) and "Approximation-2" in (20) when h_1 is estimated using pilot symbols in DCE for Rayleigh fading channels with perfect knowledge of h_2. Fig. 1 (b) compares the BERs obtained by simulation, "Exact" in (27), "Approximation-1" in (28) and "Approximation-2" in (29) when both h_1 and h_2 are estimated in DCE with $\gamma_{\varepsilon_2} = -10$ dB. One sees that the "Exact" results in (18) or (27) agree well with simulation for BPSK and 4-PAM in Fig. 1 (a) and Fig. 1 (b). The slight mismatch in low $\bar{\gamma}_1$ is caused by the numerical evaluation of the integrals for "Exact" in (18) or (27). One also sees that "Approximation-2" in (20) or (29) are close to the simulation, especially at high $\bar{\gamma}_1$. On the other hand, "Approximation-1" in (19) or (28) have larger differences from the simulation results, but they have the simplest structures. It can be seen that the approximation error is reduced by increasing $\bar{\gamma}_1$. The mismatch between "Approximation-1", "Approximation-2" and simulation is caused by the use of different approximations to "Exact" in Appendices B and C with different complexities and accuracies. Generally, all the BER curves are nearly the same and they match well with simulation when $\bar{\gamma}_1$ is above 25 dB for BPSK and above 30 dB for 4-PAM. For QPSK, similar behaviour can be observed from Fig. 1 (a) and Fig. 1 (b). However, a slight mismatch still exists between "Exact", "Approximation-1", "Approximation-2" and simulation in high $\bar{\gamma}_1$, again, due to different accuracies of the approximations used in different ranges.
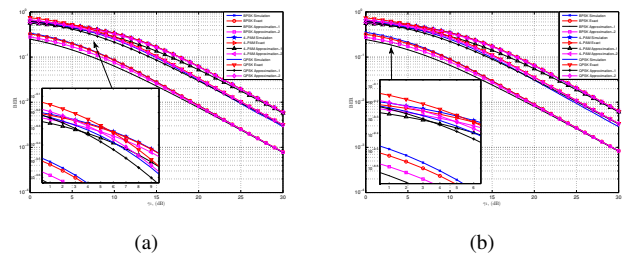

(a)   (b)

Fig. 1. BER vs. $\bar{\gamma}_1$ for AF in DCE. (a) when h_1 is estimated but with the perfect knowledge of h_2. (b) when both h_1 and h_2 are estimated with $\gamma_{\varepsilon_2} = -10$ dB.

Fig. 2 compares BERs between the case when h_1 is estimated but with perfect knowledge of h_2 and the case when both h_1 and h_2 are estimated in DCE. "Exact" in (18) and (27)

are used. It is obvious that BERs with perfect knowledge of h_2 give the best performance and with the increase of γ_{ε_2}, the BER performances of BPSK, QPSK and 4-PAM deteriorate, respectively. This is because with the deterioration of the relay-to-destination channel, the BER performances become worse accordingly.
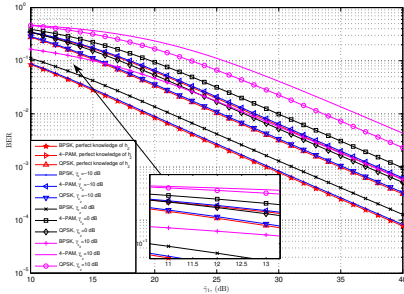

Fig. 2. Comparison of BERs between the case when h_1 is estimated but with perfect knowledge of h_2 and the case when both h_1 and h_2 are estimated in DCE.

Fig. 3 (a) compares the BERs obtained by simulation, "Exact" in (45) and "Approximation-1" in (46) when the product of h_1 and h_2 is estimated in the destination in CCE using fixed gains $G_{d_{fix_1}}$ and $G_{w_{fix_1}}$ for Rayleigh fading channels. Fig. 3 (b) compares the BERs obtained by simulation, "Exact" in (51) and "Approximation-1" in (52) in CCE using $G_{d_{fix_2}}$ and $G_{w_{fix_2}}$. $\gamma_{\varepsilon_2} = -10$ dB is set. One sees from Fig. 3 (a) and Fig. 3 (b) that there are considerable differences between "Exact" in (45) or (51), "Approximation-1" in (46) or (52) and simulation for BPSK, QPSK and 4-PAM, respectively, when $\bar{\gamma}_1$ is small. In particular, the differences between "Exact", "Approximation-1" and simulation for QPSK are the largest. Generally, when $\bar{\gamma}_1$ increases, their difference increases. That is because we assume n_w in (10) as Gaussian in order to get tractable results in CCE for BPSK, QPSK and 4-PAM. When $\bar{\gamma}_1$ increases, the approximation errors increase accordingly. Specifically, $G_{d_{fix_1}}$ and $G_{w_{fix_1}}$ are larger than $G_{d_{fix_2}}$ and $G_{w_{fix_2}}$, respectively, in the same conditions. Therefore the gap between "Exact" and simulation in Fig. 3 (a) increases quicker than the gap between "Exact" and simulation in Fig. 3 (b) when $\bar{\gamma}_1$ increases. $G_{d_{fix_1}}^2 \approx \frac{E_s}{N_1}$ and $G_{w_{fix_1}}^2 \approx \frac{E_{w_2}}{N_{w_1}}$ are used to approximate $G_{d_{fix_1}}^2$ and $G_{w_{fix_1}}^2$, respectively for "Approximation-1" in Fig. 3 (a). Interestingly, "Approximation-1" is nearly 1 dB lower than "Exact" when $\bar{\gamma}_1$ is above 15 dB such that the fitting performance of "Approximation-1" for simulation is better than "Exact" in Fig. 3 (a). But when $\bar{\gamma}_1$ is below 10 dB, "Exact" still has better performance than "Approximation-1" in Fig. 3 (a). $G_{d_{fix_2}}^2 \approx \frac{E_s}{E_d\Omega_1}$ and $G_{w_{fix_2}}^2 \approx \frac{E_{w_2}}{E_{w_1}\Omega_1}$ are used to approximate $G_{d_{fix_2}}^2$ and $G_{w_{fix_2}}^2$, respectively for "Approximation-1" in Fig. 3 (b). It is obvious that when the value of $\bar{\gamma}_1$ is large, there is no gap between "Approximation-1" and "Exact" in Fig. 3 (b). Similarly, when the value of $\bar{\gamma}_1$ is below 10 dB, "Exact" has better performance than "Approximation-1" in Fig. 3 (b). However, the use of the approximation for $G_{d_{fix_1}}$, $G_{w_{fix_1}}$, $G_{d_{fix_2}}$ and $G_{d_{fix_2}}$ can significantly simplify

the BER expressions, with slightly deteriorated performance. More importantly, these approximations do not affect the choice of the optimal power allocation obtained by using these BER expressions, as will be shown later. In other words, although these curves mismatch, their troughs with respect to the pilot power are located very close to each other.
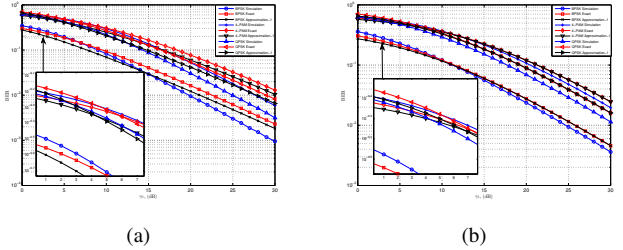

Fig. 3. BER vs. $\bar{\gamma}_1$ for AF in CCE. (a) when $G_{d_{fix_1}}$ and $G_{w_{fix_1}}$ are used. (b) when $G_{d_{fix_2}}$ and $G_{w_{fix_2}}$ are used.

B. Optimal Power Allocation Evaluation

In this part, we use the BER performance to check the optimal power values obtained from our BER expressions. "Exact" of (18) is used in DCE when h_1 is estimated, (27) is used in DCE when both h_1 and h_2 are estimated, (45) is used in CCE with the amplification gain $G_{d_{fix_1}}$, $G_{w_{fix_1}}$ and (51) is used in CCE with the amplification gain $G_{d_{fix_2}}$, $G_{w_{fix_2}}$ in Fig. 4- Fig. 8. Fig. 4 - Fig. 6 examine the optimal allocation between P_d and P_{w_1} under fixed P_1 and the optimal allocation between P_s and P_{w_2} under fixed P_2, respectively.

Fig. 4 shows the BERs vs. E_{w_1} when h_1 is estimated but with the perfect knowledge of h_2 in DCE. Fig. 5 shows the BERs vs. E_{w_1} when $G_{d_{fix_1}}$ and $G_{w_{fix_1}}$ are used in CCE. In Fig. 4 and Fig. 5, $N_1 = 1$, $N_2 = 1$, $N_{w_1} = 1$ and $N_{w_2} = 1$ are assumed. $P_1 = 30$ dB and $P_1 = 40$ dB are examined in Fig. 4 while $P_1 = 30$ dB, $P_2 = 30$ dB and $P_1 = 40$ dB, $P_2 = 40$ dB are examined in Fig. 5. Also, we set $\bar{\gamma}_2 = 30$ dB in Fig. 4 while we set $E_{w_1} = E_{w_2}$ in Fig. 5. We consider both the case when the relay is close to the source and the destination ($d_1 = 0.5$, $d_2 = 0.5$) and the case when the relay is far from the source and the destination ($d_1 = 1$, $d_2 = 1$) in Fig. 4 and Fig. 5. In these figures, the BER performances become worse when d_1 and d_2 increase (the distance between source and relay, and the distance between relay and destination, respectively). This shows that the distance between nodes and therefore the average power, have significant impact on system performance. It is understandable that if E_{w_1} (the pilot power) decreases, the BER performance will decrease even with increasing data power. This is because the system can't obtain good approximate channel information without enough pilot power. Similarly, if E_{w_1} (the pilot power) increases too much, the BER performance will also decrease even with perfect channel information. This is because the system can't perform well without enough data transmission power. This explains Fig. 4 and Fig. 5, where one can see that all the BER curves are concave and thus first decrease and then increase, when E_{w_1} (the pilot power) increases. Also, one can see from Fig. 4 and Fig. 5 that the minimum BERs are achieved at the
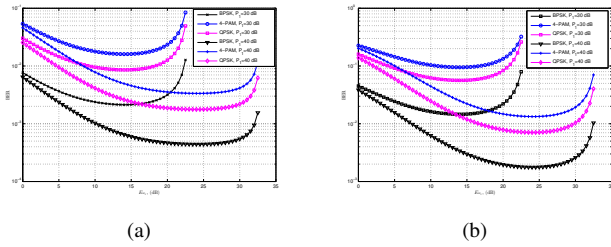
Fig. 4. BERs vs. E_{w_1} for AF in DCE when h_1 is estimated but with the perfect knowledge of h_2 with $\bar{\gamma}_2 = 30$ dB. (a) $d_1 = 0.5$, $d_2 = 0.5$. (b) $d_1 = 1$, $d_2 = 1$.
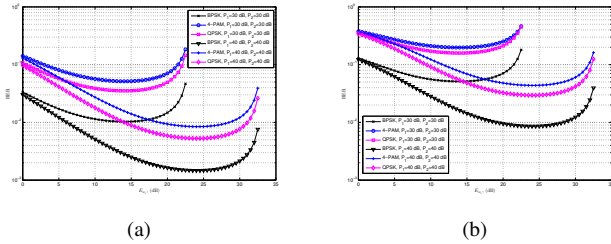

Fig. 5. BER vs. E_{w_1} for AF in CCE when $G_{d_{fix_1}}$ and $G_{w_{fix_1}}$ are used. (a) $d_1 = 0.5$, $d_2 = 0.5$. (b) $d_1 = 1$, $d_2 = 1$.

same E_{w_1} for BPSK, 4-PAM and QPSK. It proves why our optimal power allocation schemes do not include modulation-specific constants a and b such as (22), (49) and (50). The minimum BER is achieved at around $E_{w_1} = 14$ dB for $P_1 = 30$ dB and $E_{w_1} = 24$ dB for $P_1 = 40$ dB in all the BER curves for DCE in Fig. 4. From (22), one can calculate the optimal total pilot power at the source as $E_{w_1} = 14.1267$ dB for $P_1 = 30$ dB and $E_{w_1} = 24.1394$ dB for $P_1 = 40$ dB in Fig. 4 (a), while one can get optimal pilot power $E_{w_1} = 14.0257$ dB for $P_1 = 30$ dB and $E_{w_1} = 24.1295$ dB for $P_1 = 40$ dB in Fig. 4 (b). Thus, the optimal power allocation from our theoretical analysis is nearly the same as what observed from Fig. 4. Similarly, the minimum BER is achieved at around $E_{w_1} = 14$ dB for $P_1 = 30$ dB, $P_2 = 30$ dB and $E_{w_2} = 24$ dB for $P_1 = 40$ dB, $P_2 = 40$ dB in all the BER curves for CCE in Fig. 5. From (49) and (50), one can calculate $E_{w_1} = 14.1267$ dB, $E_{w_2} = 13.573$ dB for $P_1 = 30$ dB, $P_2 = 30$ dB and $E_{w_1} = 24.1394$ dB, $E_{w_2} = 23.821$ dB for $P_1 = 40$ dB, $P_2 = 40$ dB in Fig. 5 (a). One can also calculate $E_{w_1} = 14.0257$ dB, $E_{w_2} = 13.5158$ dB for $P_1 = 30$ dB, $P_2 = 30$ dB and $E_{w_1} = 24.1295$ dB, $E_{w_2} = 23.5745$ dB for $P_1 = 40$ dB, $P_2 = 40$ dB in Fig. 5 (b). Again, our theoretical value of the optimal allocation is nearly the same as that from the simulation. From Fig. 4 and Fig. 5, one can also see that the BERs with the optimal allocation have the lowest values, which implies that the power allocation proposed in this paper have better performance than all other allocation methods.

Fig. 6 compares BERs with optimal allocation between the case when h_1 is estimated but with perfect knowledge of h_2 and the case when both h_1 and h_2 are estimated in DCE. $d_1 = 1$, $d_2 = 1$, $N_1 = 1$, $N_2 = 1$, $N_{w_1} = 1$, $P_1 = P_2$ are assumed and 4-PAM modulation is examined. P_2 can be used all by data at the relay when the channel has perfect knowledge of h_2 while $N_{w_2} = 1, 10, 20, 30$ are assumed when

h_2 are estimated, where P_2 has to be shared by data and pilot by using our optimal power allocation in this case. As can be seen in Fig. 6, as P_1/H_1 (the power per symbol at the source) increases, all the BERs decrease. This is because with the total power increasing, the BER performance improves. One can also see that BERs with perfect knowledge of h_2 give the best performance and that when N_{w_2} (the noise power in pilot) increases, the BERs increase. This is because the increase of noise powers deteriorate the BER performances.
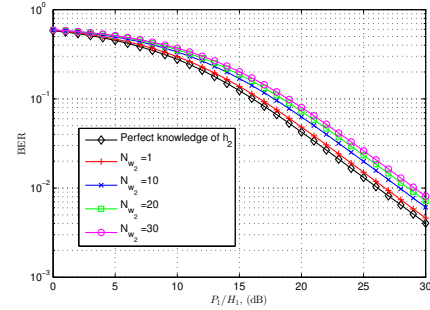

Fig. 6. Comparison of BERs with optimal allocation between the case when h_1 is estimated but with perfect knowledge of h_2 and the case when both h_1 and h_2 are estimated in DCE.

In Fig. 7 and Fig. 8, we compare the BER using the optimal power allocation between P_d, P_s, P_{w_1}, P_{w_2} under fixed P_T with the BER using equal power allocation without optimization where $P_d = \frac{P_T D}{H}$, $P_s = \frac{P_T D}{H}$, $P_{w_1} = \frac{P_T W_1}{H}$ and $P_{w_2} = \frac{P_T W_2}{H}$. We set $d_2 = 1$ and $N_1 = 1$ in Fig. 7 and Fig. 8. 4-PAM modulation is used as examples and other modulation can be checked in a similar way.

Fig. 7 shows the BERs vs. P_T/H when both h_1 and h_2 are estimated in DCE. Fig. 8 shows the BERs vs. P_T/H when $G_{d_{fix_2}}$ and $G_{w_{fix_2}}$ are used in CCE. d_1 is decreased from $1/4$ d_2 in Fig. 7 (a) and Fig. 8 (a) to $1/10$ d_2 in Fig. 7 (b) and Fig. 8 (b), respectively. From Fig. 7 and Fig. 8, one can see that the BERs with optimal power allocation outperform the BERs with equal allocation under the same conditions. Comparing the system with $N_{w_2} = N_{w_1} = N_2 = N_1$ in Fig. 7 (a) and Fig. 7 (b), one can see that the BER improves when d_1 (the distance between source and relay) decreases. This is because when d_1 decreases, the average power increases and thus, the BER performance improves. Also, in this case, as d_1 is decreased from $1/4$ d_2 in Fig. 7 (a) to $1/10$ d_2 in Fig. 7 (b), the performance gain of optimal allocation over equal allocation is increased from 2 dB to 3 dB. This is because equal allocation can not perform well when the status of source-to-relay channel is different from that of the relay-to-destination channel. Therefore, with the decrease of d_1, the difference between d_1 and d_2 becomes larger such that the performance gain will increase accordingly. As can be seen in Fig. 7 (a), with the increase of N_{w_2} and N_2 from N_1 to $3N_1$, the performance gain increases from 2 dB to 2.25 dB. Also, with the increase of N_{w_2} and N_{w_1} from N_1 to $3N_1$, the performance gain increases from 2 dB to 2.4 dB. This is also because that with the increase of difference of noise power between source-to-relay and relay-to-destination channel or between data transmission and pilot transmission,

the performance gain increases. In Fig. 7 (b), as the increase of N_{w_2} and N_{w_1} from $10N_1$ to $20N_1$, the performance gain increases from 4.8 dB to 5.5 dB with the same reason above. Similar analysis and conclusion can be made from Fig. 8
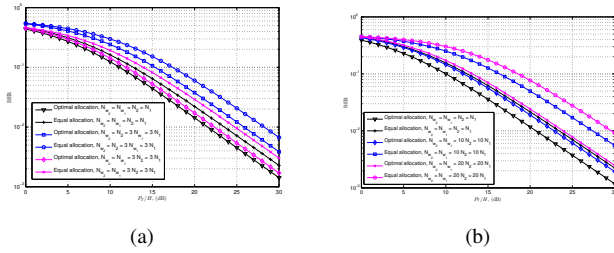

(a)   (b)

Fig. 7. BER vs. P_T/H for AF in DCE when both h_1 and h_2 are estimated. (a) $d_1 = 1/4\ d_2$. (b) $d_1 = 1/10\ d_2$.

(a) and Fig. 8 (b) in CCE. Moreover, when setting $d_1 = 1$, $d_2 = 1/4\ d_1$ and $d_2 = 1/10\ d_1$ in Fig. 7 and Fig. 8, similar performance gain can be obtained.
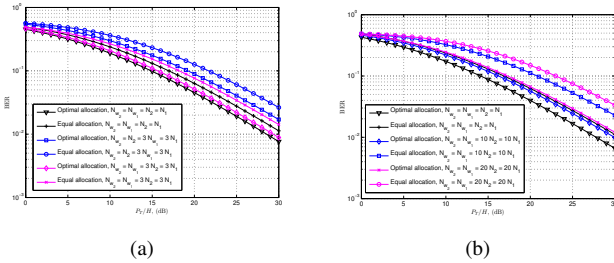

(a)   (b)

Fig. 8. BER vs. P_T/H for AF in CCE when $G_{d_{fix_2}}$ and $G_{w_{fix_2}}$ are used. (a) $d_1 = 1/4\ d_2$. (b) $d_1 = 1/10\ d_2$.

VI. CONCLUSION

The BER and the outage probability of AF relaying systems using variable gain in DCE and fixed gains in CCE have been derived when different channel gains are estimated using the pilot-aided ML estimation for slowly fading Rayleigh channels. Based on these BERs, two kinds of optimal power allocation have been studied. From the derivation, one can see that the BER expressions for CCE are more complex than those for DCE, as they include the Meijer's G - function. This paper considers a single carrier system. The optimization only needs to be done once using channel statistics and can be offline. An interesting future work is to extend it to multi-carrier systems with higher spectral efficiency, provided that closed-form expressions for BER can be obtained.

APPENDIX

A. Derivation of (17)

The cumulative distribution function (CDF) of the end-to-end SNR in (16) can be derived as

$$F_{\gamma_{end_1}}(\gamma_{th}) = \int_0^\infty P\left(\frac{\gamma_2\hat{\gamma}_1}{\gamma_2 + \hat{\gamma}_1 + 1 + \gamma_{\varepsilon_1}\gamma_2} \le \gamma_{th}|\gamma_2\right)$$
$$\times f(\gamma_2)d\gamma_2 = 1 - \int_{\gamma_{th}}^\infty e^{-\frac{\gamma_{th}\gamma_2 + \gamma_{th} + \gamma_{\varepsilon_1}\gamma_{th}\gamma_2}{\hat{\gamma}_1(\gamma_2 - \gamma_{th})}} f(\gamma_2)d\gamma_2.$$
$$(61)$$

By using $z = \gamma_2 - \gamma_{th}$, one has.

$$F_{\gamma_{end_1}}(\gamma_{th}) = 1-$$
$$\frac{1}{\bar{\gamma}_2}\int_0^\infty e^{-\frac{(z+\gamma_{th})\gamma_{th} + \gamma_{th} + (z+\gamma_{th})\gamma_{th}\gamma_{\varepsilon_1}}{\hat{\gamma}_1 z} - \frac{z+\gamma_{th}}{\bar{\gamma}_2}}dz.$$
$$(62)$$

Using [26, (3.471)], the CDF can be derived as (17).

B. Derivation of (19)

In the asymptotic case, we have $\bar{\hat{\gamma}}_1, \bar{\gamma}_2 \to \infty$. Using the approximation of [26]

$$K_\nu(x) \approx \frac{2^{\nu-1}\Gamma(\nu)}{x} \tag{63}$$

in (17), one has

$$F_{\gamma_{end_1}}(\gamma_{th}) \approx 1 - e^{-\gamma_{th}\beta_2}. \tag{64}$$

Then using (18) and (64), one can obtain the approximate BER as (19).

C. Derivation of (20)

When γ_{ε_1} is large, we have $\gamma_{\varepsilon_1}\gamma_{th} + \gamma_{th} + 1 \approx \gamma_{\varepsilon_1}\gamma_{th} + \gamma_{th}$. Then (17) can be approximated as

$$F_{\gamma_{end_1}}(\gamma_{th}) \approx 1 - \beta_1\gamma_{th}e^{-\gamma_{th}\beta_2}K_1(\gamma_{th}\beta_1). \tag{65}$$

One can use (65) in (18) with [26, (6.621)] to solve the integral as (20).

D. Derivation of (26)

The CDF of the end-to-end SNR in (25) can be written as

$$F_{\gamma_{end_2}}(\gamma_{th}) = \int_0^\infty$$
$$P\left(\frac{\hat{\gamma}_2\hat{\gamma}_1}{\hat{\gamma}_2\gamma_{\varepsilon_1} + \hat{\gamma}_1\gamma_{\varepsilon_2} + \gamma_{\varepsilon_1}\gamma_{\varepsilon_2} + \hat{\gamma}_2 + \hat{\gamma}_1 + 1 + \gamma_{\varepsilon_2}} \le \gamma_{th}|\hat{\gamma}_2\right)$$
$$\times f(\hat{\gamma}_2)d\hat{\gamma}_2$$
$$= 1 - \int_{\gamma_{th}}^\infty e^{-\frac{\hat{\gamma}_2(\gamma_{th}\gamma_{\varepsilon_1} + \gamma_{th}) + \gamma_{\varepsilon_1}\gamma_{\varepsilon_2}\gamma_{th} + \gamma_{\varepsilon_2}\gamma_{th} + \gamma_{th}}{\hat{\gamma}_1(\hat{\gamma}_2 - \gamma_{\varepsilon_2}\gamma_{th} - \gamma_{th})}} f(\hat{\gamma}_2)d\hat{\gamma}_2.$$
$$(66)$$

Let $z = \hat{\gamma}_2 - \gamma_{\varepsilon_2}\gamma_{th} - \gamma_{th}$ and using [26, (3.471)], the CDF can be derived as (26).

E. Derivation of (43)

By substituting $\hat{H}$ with $\hat{H}^2$ in (12), one can get the PDF of $\hat{H}^2$ as

$$f_{\hat{H}^2}(x) = \frac{2K_0\left(2\sqrt{\frac{x}{\Omega}}\right)}{\Omega}, \ x > 0. \tag{67}$$

Then, one can get the CDF of $\hat{H}^2$ as

$$F_{\hat{H}^2}(y) = 1 - 2\sqrt{\frac{y}{\Omega}}K_1\left(2\sqrt{\frac{y}{\Omega}}\right). \tag{68}$$

Using (42), $\hat{H}^2$ can be written as

$$\hat{H}^2 = \frac{\gamma_{fix}(E_d\Omega_\varepsilon G_{d_{fix_1}}^2 + N)}{E_d G_{d_{fix_1}}^2}. \tag{69}$$

Then, using (68) and (69), the outage probability can be derived as (43).

REFERENCES

[1] J. N. Laneman and G. W. Wornell, "Energy-efficient antenna sharing and relaying for wireless networks," in *IEEE Confernce on Wireless Communications and Networking (WCNC'2000)*, 2000, pp. 7–12.

[2] J. N. Laneman, G. W. Wornell, and D. Tse, "An efficient protocol for realizing cooperative diversity in wireless networks," in *IEEE International Symposium on Information Theory (ISIT'2001)*, 2001, p. 294.

[3] M. O. Hasna and M.-S. Alouini, "A performance study of dual-hop transmissions with fixed gain relays," *IEEE Transactions on Wireless Communications*, vol. 3, no. 6, pp. 1963 – 1968, Nov. 2004.

[4] ——, "End-to-end performance of transmission systems with relays over Rayleigh-fading channels," *IEEE Transactions on Wireless Communications*, vol. 2, no. 6, pp. 1126 – 1131, Nov. 2003.

[5] O. Amin, B. Gedik, and M. Uysal, "Channel estimation for amplify-and-forward relaying: Cascaded against disintegrated estimators," *IET Communications*, vol. 4, no. 10, pp. 1207 –1216, Jul. 2010.

[6] F. A. Khan, Y. Chen, and M.-S. Alouini, "Novel receivers for af relaying with distributed stbc using cascaded and disintegrated channel estimation," *IEEE Transactions on Wireless Communications*, vol. 11, no. 4, pp. 1370 –1379, Apr. 2012.

[7] C. S. Patel and G. L. Stuber, "Channel estimation for amplify and forward relay based cooperation diversity systems," *IEEE Transactions on Wireless Communications*, vol. 6, no. 6, pp. 2348 –2356, Jun. 2007.

[8] F. Gao, T. Cui, and A. Nallanathan, "On channel estimation and optimal training design for amplify and forward relay networks," *IEEE Transactions on Wireless Communications*, vol. 7, no. 5, pp. 1907 –1916, May. 2008.

[9] H. Mheidat and M. Uysal, "Non-coherent and mismatched-coherent receivers for distributed stbcs with amplify-and-forward relaying," *IEEE Transactions on Wireless Communications*, vol. 6, no. 11, pp. 4060 – 4070, Nov. 2007.

[10] J. G. Proakis and M. Salehi, *Digital Communications*. New York: McGraw-Hill, 2008.

[11] L. Tong, B. M. Sadler, and M. Dong, "Pilot-assisted wireless transmissions: general model, design criteria, and signal processing," *IEEE Signal Processing Magazine*, vol. 21, no. 6, pp. 12 – 25, Nov. 2004.

[12] Y. Wu and M. Patzold, "Parameter optimization for amplify-and-forward relaying with imperfect channel estimation," in *IEEE 69th Vehicular Technology Conference*, 2009, pp. 1–5.

[13] M. Mohammadi, P. Sadeghi, and M. Ardebilipour, "Node and symbol power allocation in time-varying amplify-and-forward dual-hop relay channels," *IEEE Transactions on Vehicular Technology*, vol. 62, no. 1, pp. 432–439, 2013.

[14] A. Lalos, A. Rontogiannis, and K. Berberidis, "Frequency domain channel estimation for cooperative communication networks," *IEEE Transactions on Signal Processing*, vol. 58, no. 6, pp. 3400–3405, June 2010.

[15] Y. Gao, D. Lin, B. Li, and S. Li, "Optimal training power allocation for amplify and forward relay networks," in *2010 International Conference on Communications, Circuits and Systems (ICCCAS)*, 2010, pp. 73–77.

[16] B. Gedik, O. Amin, and M. Uysal, "Power allocation for cooperative systems with training-aided channel estimation," *IEEE Transactions on Wireless Communications*, vol. 8, no. 9, pp. 4773–4783, 2009.

[17] H. Rasouli and A. Anpalagan, "SNR-based vs. BER-based power allocation for an amplify-and-forward single-relay wireless system with mrc at destination," in *2010 25th Biennial Symposium on Communications (QBSC)*, 2010, pp. 429–432.

[18] F. Tabataba, P. Sadeghi, and M.-R. Pakravan, "Outage probability and power allocation of amplify and forward relaying with channel estimation errors," *IEEE Transactions on Wireless Communications*, vol. 10, no. 1, pp. 124–134, 2011.

[19] J. Cavers, "An analysis of pilot symbol assisted modulation for rayleigh fading channels [mobile radio]," *IEEE Transactions on Vehicular Technology*, vol. 40, no. 4, pp. 686–693, Nov. 1991.

[20] G. Colavolpe and R. Raheli, "Noncoherent sequence detection in frequency nonselective slowly fading channels," *IEEE Journal on Selected Areas in Communications*, vol. 18, no. 11, pp. 2302–2311, Nov. 2000.

[21] V. Tarokh, N. Seshadri, and A. Calderbank, "Space-time codes for high data rate wireless communication: performance criterion and code construction," *IEEE Transactions on Information Theory*, vol. 44, no. 2, pp. 744–765, Mar. 1998.

[22] Y. Chen and N. Beaulieu, "Maximum likelihood estimation of SNR using digitally modulated signals," *IEEE Transactions on Wireless Communications*, vol. 6, no. 1, pp. 210–219, 2007.

[23] B. Hassibi and B. Hochwald, "How much training is needed in multiple-antenna wireless links?" *IEEE Transactions on Information Theory*, vol. 49, no. 4, pp. 951–963, 2003.

[24] R. U. Nabar, H. Bolcskei, and F. W. Kneubuhler, "Fading relay channels: Performance limits and space-time signal design," *IEEE Journal on Selected Areas in Communications*, vol. 22, no. 6, pp. 1099 – 1109, Aug. 2004.

[25] M. K. Simon, *Probability Distributions Involving Gaussian Random Variables: A Handbook for Engineers and Scientists*. Boston, MA: Kluwer, 2002.

[26] I. S. Gradshteyn and I. M. Ryzhik, *Table of Integrals, Series, and Products, 7th ed.* San Diego, CA: Academic, 2007.

[27] Y. Chen and C. Tellambura, "Distribution functions of selection combiner output in equally correlated Rayleigh, Rician, and Nakagami-m fading channels," *IEEE Transactions on Communications*, vol. 52, no. 11, pp. 1948–1956, 2004.

Kezhi Wang (S'14) received his B.E. and M.E. degrees in College of Automation from Chongqing University, P.R.China, in 2008 and 2011, respectively. He is currently a Ph.D. student at School of Engineering in University of Warwick, U.K., from Oct. 2011. His research interests include wireless relaying, channel estimation and modelling.

Yunfei Chen (S'02-M'06-SM'10) received his B.E. and M.E. degrees in electronics engineering from Shanghai Jiaotong University, Shanghai, P. R. China, in 1998 and 2001, respectively. He received his Ph.D. degree from the University of Alberta in 2006. He is currently working as an Associate Professor at the University of Warwick, U.K. His research interests include cognitive radio, wireless relaying, and performance analysis.

Mohamed-Slim Alouini (S'94, M'98, SM'03, F'09) was born in Tunis, Tunisia. He received the Ph.D. degree in Electrical Engineering from the California Institute of Technology (Caltech), Pasadena, CA, USA, in 1998. He served as a faculty member in the University of Minnesota, Minneapolis, MN, USA, then in the Texas A&M University at Qatar, Education City, Doha, Qatar before joining King Abdullah University of Science and Technology (KAUST), Thuwal, Makkah Province, Saudi Arabia as a Professor of Electrical Engineering in 2009. His current research interests include the modeling, design, and performance analysis of wireless communication systems.

Feng Xu received his B.E. and M.E. degrees in College of Computer and Information Engineering from Hohai University, Nanjing, P. R. China, in 1998 and 2002, respectively. He received his Ph.D. degree from Nanjing University in 2008. He is currently working as a Professor at Hohai University, P.R.China. His research interests include network security, cloud computing, and wireless communications theory.